Available online at www.sciencedirect.com
ScienceDirect
Solar Energy 82 (2008) 977–985
SOLAR ENERGY
www.elsevier.com/locate/solener

Numerical and experimental investigation for heat transfer in triplex concentric tube with phase change material for thermal energy storage

Long Jian-you *

Shunde Polytechnic College, Foshan Guangdong 528333, China

Received 8 August 2006; received in revised form 8 May 2008; accepted 10 May 2008
Available online 13 June 2008

Communicated by: Associate Editor Halime Paksoy

Abstract

This paper addresses a numerical and experimental investigation of a thermal energy storage unit involving phase change process dominated by heat conduction. The thermal energy storage unit involves a triplex concentric tube with phase change material (PCM) filling in the middle channel, with hot heat transfer fluid (HHTF) flowing outer channel during charging process and cold heat transfer fluid (CHTF) flowing inner channel during discharging process. A simple numerical method according to conversation of energy, called temperature & thermal resistance iteration method has been developed for the analysis of PCM solidification and melting in the triplex concentric tube. To test the physical validity of the numerical results, an experimental apparatus has been designed and built by which the effect of the inlet temperature and the flow rate of heat transfer fluid (HTF, including HHTF and CHTF) on the thermal energy storage has been studied. Comparison between the numerical predictions and the experimental data shows good agreement. Graphical results including fluid temperature and interface of solid and liquid phase of PCM versus time and axial position, time-wise variation of energy stored/released by the system were presented and discussed.

Keywords: Phase change material; Energy storage; Concentric tube; Heat transfer

1. Introduction

Energy resources on the earth will be exhausted one day if they are used in an unchecked way. This will cause serious problems and even crisis and jeopardize the survival of mankind. In China, with the rapid development of economy and the much improvement of people's living standard, the problem of energy shortage becomes serious. Especially after early morning until midnight, this problem becomes more serious for more power consumption of industrial, commercial and residential activities during that period of time.

There are two ways to relieve this serious situation to some extent. One is to shift electricity usage from peak periods to off peak periods. The other is to recover the energy which is used to be ejected directly to the environment as wasted heat such as the ejected heat from the condenser of air conditioner, or to collect and utilize the diurnally fluctuating thermal energy such as the solar energy. In any case, an energy storage system should be necessary.

Due to worldwide energy shortage, the development of efficient and cost effective thermal storage system has received considerable attention due to the impending shortage and increasing cost of energy resources (Hamada, 2003). A thermal storage system is expected to provide to timely and complete energy management by excessive thermal energy at energy-rich periods to utilize it at

* Tel.: +86 0757 28925751; fax: +86 0757 22326903.
E-mail address: jianyoulong@163.com

0038-092X/$ - see front matter © 2008 Elsevier Ltd. All rights reserved.
doi:10.1016/j.solener.2008.05.006

Nomenclature

C_p	heat capacity (J kg^{-1} K^{-1})	*Greek symbols*	
D	diameter of the tube (m)	α	convective heat transfer coefficient (W m^{-2} K^{-1})
H	phase change latent heat (kJ m^{-3})	λ	thermal conductivity (W m^{-1} K^{-1})
m	mass flow rate (kg s^{-1})		
Q	heat transfer rate (kW)	*Subscripts*	
R	thermal resistance (m K W^{-1})	f	HTF
r	coordinate along the radial direction (m)	i	inlet
T	temperature difference (K)	m	phase change material
t	time(s)	o	outlet
x	coordinate along the axial direction (m)	w	wall

energy-poor periods. The main task of the energy storage is then to overcome the discrepancies between energy supply and energy demand. There are three main methods of thermal energy storing: sensible, latent and thermal–chemical heat storage. A latent thermal energy storage system, with solid–liquid phase change, has received a considerable attention due to its advantages, such as storing a large amount of energy in a small volume i.e., high storage density and heat charging/discharging at a nearly constant temperature, which result in a greater flexibility and more compactness of the PCM storage system in choosing a location for the storage system (Setterwall, 1996).

Experiments have been conducted to study the thermal performance of PCM storage systems and numerous publications have been found (Banaszek et al., 2000; Al Hallaj and Selman, 2000; Neeper, 2000; Py et al., 2001; Liu and Chung, 2001). According to these publications, paraffin waxes have been extensively used as PCM for many applications. This is because not only paraffin waxes are nonpoisonous, non-corrosive, chemically stable, relatively high latent heat capacity, but also they have a negligible degree of subcooling during nucleation, no phase separation and only a small volume change in the phase change process.

In this paper, a triplex concentric tube with HHTF flowing outer channel, CHTF flowing inner channel and PCM filling in the middle channel was designed for energy recovery of wasted heat in industry, ejected heat from the condenser of air conditioner or solar energy.

Report about heat transfer of triplex concentric tube with phase change material for thermal energy storage has not appeared so far. Only phase change heat transfer of dual concentric tube or shell-and-tube for thermal energy storage can be found for reference. Heat transfer in these types of thermal energy storage system represents a transient conjugate phase change-forced convection problem. Since phase change heat transfer is non-linear due to the moving solid–liquid interface, analytical solutions are only known for a few so-called moving boundary problems with simple geometry and simple boundary conditions. Therefore, a numerical approach has to be used to achieve a sufficiently accurate solution for heat transfer in the latent thermal energy storage unit. The most common methods used for solving phase change problems are the enthalpy methods and temperature-based equivalent heat capacity methods. These methods have been used in mathematical approaches by many authors (Zhang and Faghri, 1996; Ismail and Abugderah, 2000; Zivkovic and Fujii, 2001; Sari and Kaygusuz, 2002; Kayansayan and Ali Acar, 2006).

Although so many researchers focus on the problem of phase change of PCM as mentioned above, their models are still too complex and need huge workload of calculation. In this paper, a simple numerical method, called temperature & thermal resistance iteration method, has been developed for the analysis of PCM solidification and melting in the triplex concentric tube. To test the physical validity of the numerical results, an experimental apparatus has been designed and built by which the effect of the inlet temperature and the flow rate of HTF on the thermal energy storage has been studied. From the point of view of application, the variations of heat transfer rate, fluid temperature, the front movement during solidification and melting with time are important quantities to study the characteristics of latent heat thermal storage. So graphical results including fluid temperature and interface of solid and liquid phase of PCM versus time and axis position, time-wise variation of energy stored/released by the system were presented and discussed.

2. Experiment equipment and test procedure

2.1. Experimental setup

A schematic diagram of experimental setup is shown in Fig. 1.

The experimental system consists of a triplex concentric tube with PCM filling in the middle channel, a constant temperature circulating bath, a flow meter, a variable speed pump, and a return piping for the HTF. The PCM selected for the present study is *n*-Hexacosane and it is suitable for the domestic hot water system. Table 1 summarizes the thermophysical properties of the *n*-Hexacosane given by Zhang et al. (1996). To reduce the heat lose to the environment, the outer wall of the triplex concentric tube is

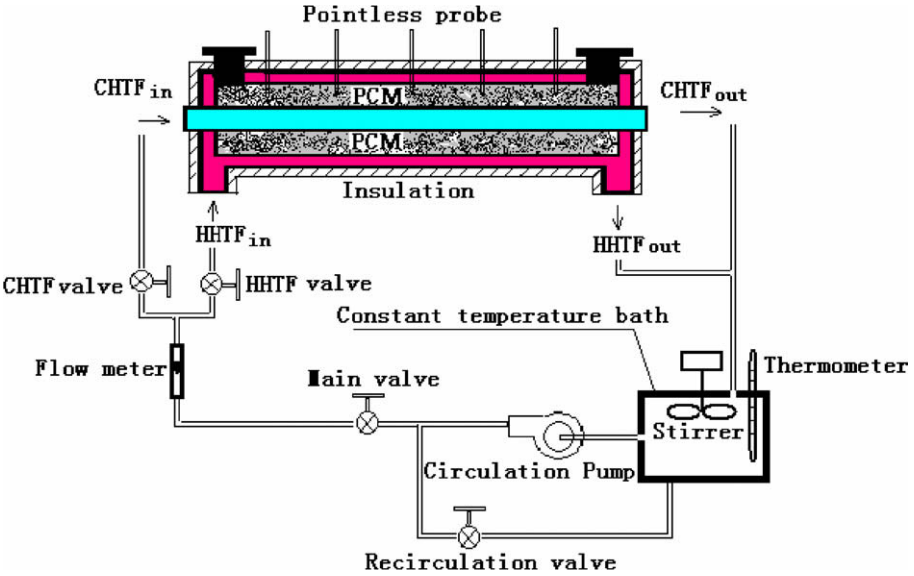

Fig. 1. Schematic diagram of experimental setup.

Table 1
Thermophysical properties of the *n*-Hexacosane

Melting/solidification temperature	56.3 °C
Latent heat capacity	61 kcal kg^{-1}
Thermal conductivity	0.22 W m^{-1} K^{-1}
Density	0.77 g ml^{-1}

insulated with 20 mm thick Styrofoam layer. To set the inlet temperature of HTF to a desired value and control the flow rate, the apparatus contains several valves. Additionally, the entire piping is insulated with a 20 mm thick Styrofoam layer.

The triplex concentric tube consists of three tubes as shown in Fig. 3. All the tubes are made of copper. The inner one has the length of 3100 mm with the inner and outer diameter of 15 mm and 17 mm, respectively. The middle one has the length of 3000 mm with the inner and outer diameter of 80 mm and 82 mm, respectively. The outer one has the length of 3040 mm with the inner and outer diameter of 90 mm and 94 mm, respectively. The HTF flows by forced convection through the inner or outer tube. A pointless probe was used to examine the interface between the liquid and solid phase during the process of solidification and melting through the little hole on the middle tube.

The HTF is distilled water. A constant temperature bath with a sensitivity of ±0.1 °C is used in providing the desired temperature of HTF at the inlet of the test section. A variable speed pump circulates the HTF through the flow system. The HTF is metered by a glass tube variable area rotameter with a sensitivity of 0.05 L min^{-1} and a maximum capacity 2 L min^{-1}. The inlet and outlet temperature of HTF is measured by copper-constant thermocouples (Type T) with a sensitivity of 0.1 °C, calibrated by a precision thermometer. All thermocouples were connected to the data acquisition system YOKOGAWA DR130 (20 Points).

2.2. Experimental procedure

Prior to the experimentation, *n*-Hexacosane in the test section was heated to a temperature slightly higher than its melting point by circulating water of 58 °C. The solidification experiment was then started with established initial conditions. Cole water (as CHTF) was drained from the constant temperature bath with a constant mass flow rate and temperature below the solidification temperature range, started to circulate. Inlet and outlet temperature of CHTF were measured and recorded. At the same time, the pointless probe was put in the little hole on the middle tube to examine the solidification front during the process of solidification every 10 min. The solidification experiment was completed when the *n*-Hexacosane at the end of the test section was completely solidified.

The melting experiment started immediately after the solidification experiment. Hot water (as HHTF) from the constant temperature bath at a required temperature, over the melting range, started to circulate and data collection began. Inlet and outlet temperature of HTF were measured and recorded. And the melting front during the process of melting was also examined by the pointless probe during the process of melting every 10 min. When the *n*-Hexacosane at the end of the test section was completely melted, the melting experiment was finished.

2.3. Experimental results

2.3.1. Solidification (discharging) process

Several *n*-Hexacosane solidification experiments were performed for different mass flow rates and inlet temperatures of the cold water. Comparison between the numerical

predictions and the experimental data of inlet and outlet temperature of CHTF and solidification front distribution shows good agreement, as shown in Figs. 2 and 3.

2.3.2. Melting (charging) process

Several *n*-Hexacosane melting experiments were also performed for different mass flow rates and inlet temperatures of the HHTF. Comparison between the numerical predictions and the experimental data of inlet and outlet temperature of HHTF and solidification front distribution also shows good agreement, as shown in Figs. 4 and 5.

Experimental data have been compared with the calculated numerical predictions. By comparison of predictions with experimental data, the physical validity of the numerical model below has been studied. It can be seen from the figures that the numerical predictions coincide quite well with the experimental results. The minor discrepancies between the numeration and measurements can be ascribed to the measurements uncertainties and model simplifications. The results obtained pointed out that a presented numerical procedure could be accurately used for transient heat transfer simulation in a triplex concentric tube latent thermal energy storage unit during charging and discharging.

3. Modeling of the thermal energy storage unit and numerical solution

3.1. Thermal energy storage unit

The thermal energy storage unit involves a triplex concentric tube with PCM filling in the middle channel, with HHTF flowing outer channel during charging (melting) process and CHTF flowing inner channel during discharging (solidification) process, as shown in Fig. 6.

3.2. Numerical procedure

3.2.1. Assumptions

In developing the conduction model for the thermal energy storage unit, the following assumptions are made.

(1) The thermophysical properties of the liquid and the solid phase of PCM are the same. All the properties remain constant with respect to temperature.

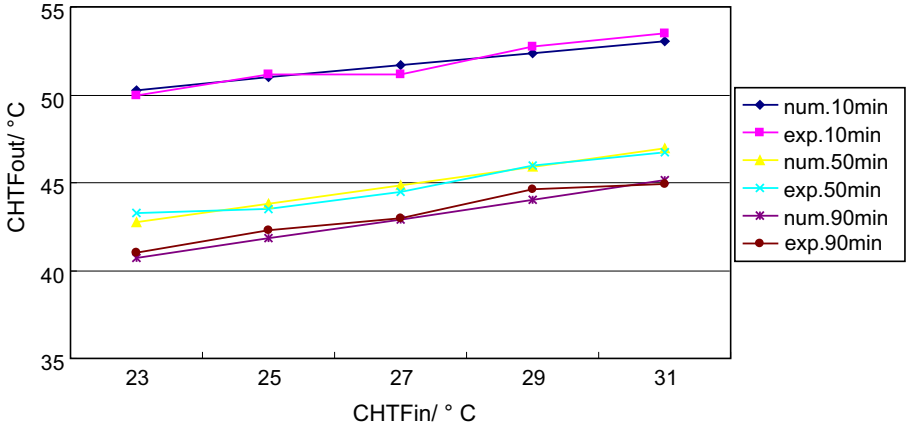

Fig. 2. Comparison of experiment and numeration during solidification.

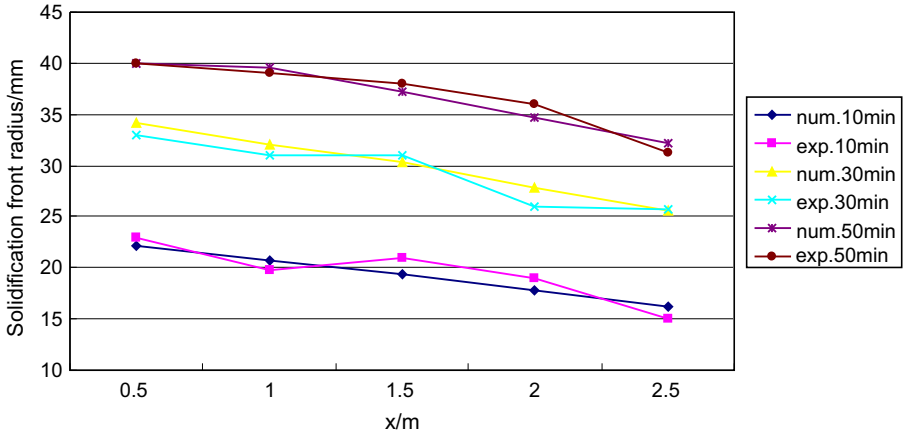

Fig. 3. Comparison of experiment and numeration during solidification.

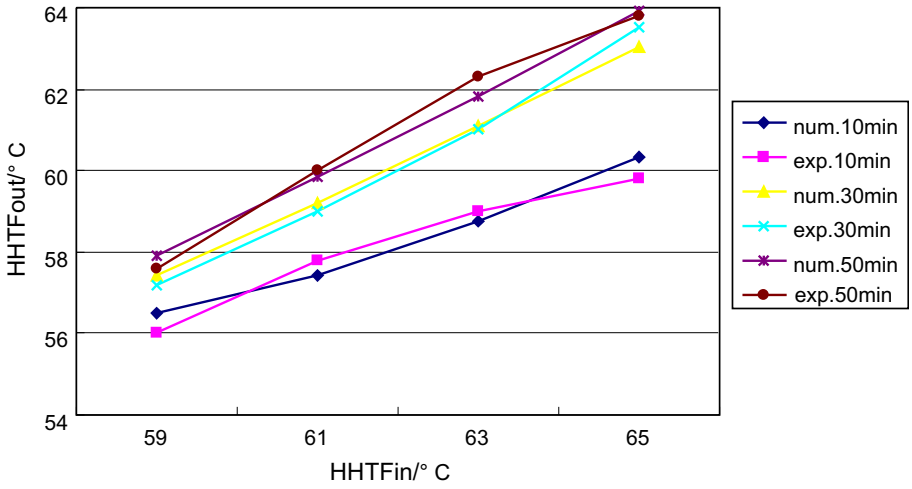

Fig. 4. Comparison experiment and numeration during melting.

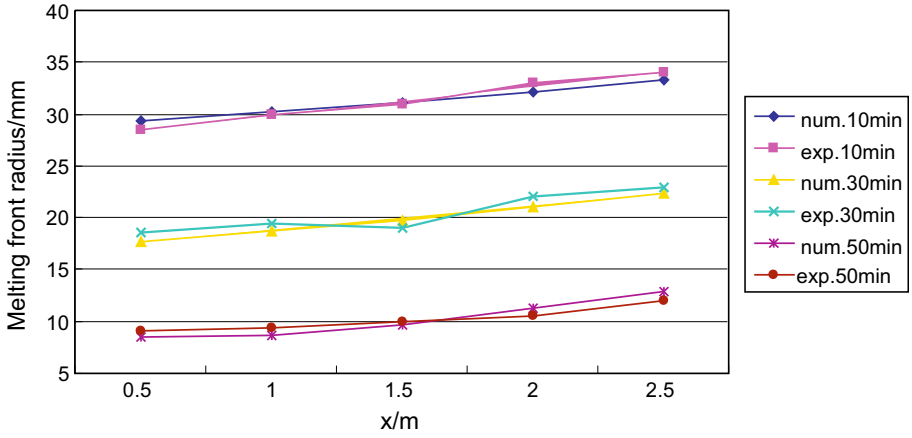

Fig. 5. Comparison of experiment and numeration during melting.

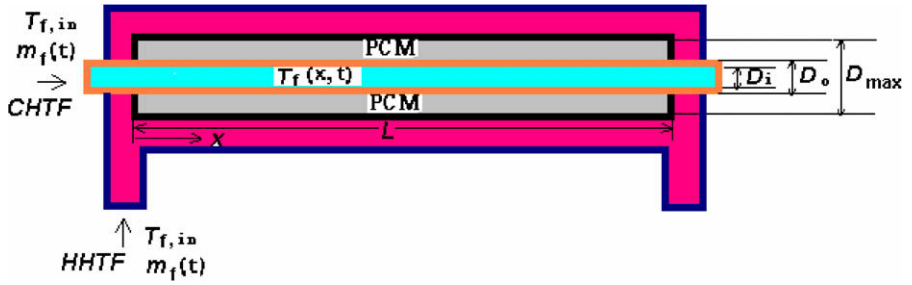

Fig. 6. Schematic diagram of the thermal energy storage unit.

(2) The buoyancy force from volume change due to phase change is ignored. The effect of natural convection in the liquid phase of PCM is not taken into account.
(3) The conduction in the PCM and tube wall is circumferential, and the conduction in axial direction is neglected. The problem is axisymmetric.
(4) Initial temperature of the thermal energy storage unit is uniform.
(5) Adiabatic outer wall is assumed.

3.2.2. Equations for heat transfer model

The following is the numerical solution procedure for solidification.

According to these simplifications above and conversation of energy, heat transfer process between the CHTF and PCM during solidification can be described as following equations (Zhang et al., 1996):

$$\alpha_f \pi D_i [T_w(x,t) - T_f(x,t)] = C_{p,f} m_f(t) \frac{\partial T_f(x,t)}{\partial x} \quad (1)$$

$$\alpha_f \pi D_i [T_w(x,t) - T_f(x,t)] = 2\pi H_m r_m(x,t) \frac{\partial r_m(x,t)}{\partial t} \quad (2)$$

$$\frac{[T_w(x,t) - T_f(x,t)]}{T_m - T_f(x,t)} = \frac{R_\alpha}{R_\alpha + R_w + R_m(x,t)} \quad (3)$$

Here, T_f and T_w represent the local temperature of the fluid and the local temperature of the tube inner wall, respectively. They are the function of x and t. H_m and T_m represent latent heat and the phase change temperature of PCM, respectively. $R_\alpha = \frac{1}{\alpha_f}$, $R_w = \frac{D_i}{2\lambda_w} \ln \frac{D_o}{D_i}$, and $R_m(x,t) = \frac{D_i}{2\lambda_m} \ln \frac{D_m(x,t)}{D_o}$ represent the convective thermal resistance of HTF, conductive thermal resistance of tube wall and PCM.

3.2.3. Initial and boundary conditions

(1) Initial condition:

$$r_m(x, t=0) = r_o \quad (4)$$

$$T_f(x, t=0) = T_m \quad (5)$$

(2) Boundary condition:

$$T_f(x=0, t) = T_{in}(t) \quad (6)$$

3.2.4. Solution to the equations

According to Formula (1) and (3), the Formula (7) and (8) is obtained. And according to Formula (2) and (3), the Formula (9) and (10) is obtained

$$\frac{\partial T_f(x,t)}{\partial x} = \frac{\pi D_i \alpha_f}{C_{P,f} m_f(t)} \times \frac{R_\alpha}{R_\alpha + R_w + R_m(x,t)} \times [T_m - T_f(x,t)] \quad (7)$$

$$T_f(x,t) = T_m - [T_m - T_{in}(t)] \times \exp\left[-\frac{\pi D_i \alpha_f}{C_{P,f} m_f(t)} \times \frac{R_\alpha}{R_\alpha + R_w + R_m(x,t)} \times x \right] \quad (8)$$

$$\frac{\partial r_m^2(x,t)}{\partial t} = \frac{\alpha_f D_i}{H_m} \times \frac{R_\alpha}{R_\alpha + R_w + R_m(x,t)} \times [T_m - T_f(x,t)] \quad (9)$$

$$r_m(x,t) = \sqrt{r_0^2 + \int_0^t \frac{\alpha_f D_i}{H_m} \times \frac{R_\alpha}{R_\alpha + R_w + R_m(x,t)} \times [T_m - T_f(x,t)] dt} \quad (10)$$

Iteration method (called temperature & thermal resistance iteration method by (Kang et al., 1999) could be used to obtain the solutions of Formula group (8) and (10). Then the distributions of temperature of HTF and solidification front of PCM were gained.

Numerical solution for melting has the same procedure of solidification, except that the heat transfer area is the outer surface of middle tube, not the inner surface of the inner tube (as shown in Fig. 6). So the numerical solution procedure for melting is not given here.

3.3. Numerical results and discussion

3.3.1. Front distribution of PCM

The solidification and melting front variation of PCM with time at the different axial position is shown in Figs. 7 and 8, respectively.

With the inlet fluid temperature at 23 °C, the solidification front radius of PCM at different axial position increases with increasing time, as shown in Fig. 7. Time for complete solidification at the entrance, middle and end of the tube is about 40, 50 and 100 min, respectively, and the velocity of solidification front going forward decreases with increasing time for the gradually increased conductive thermal resistance of PCM.

And with the inlet fluid temperature at 65 °C, the melting front radius of PCM at different axial position decreases with increasing time as shown in Fig. 8.

3.3.2. Temperature distribution

The temperature variation of *CHTF* and HHTF with time at different axial position is shown in Figs. 9 and 10, respectively.

With the inlet fluid temperature at 23 °C, the temperature of CHFT at different axial position sharply fist, then slowly decreases with increasing time due to the

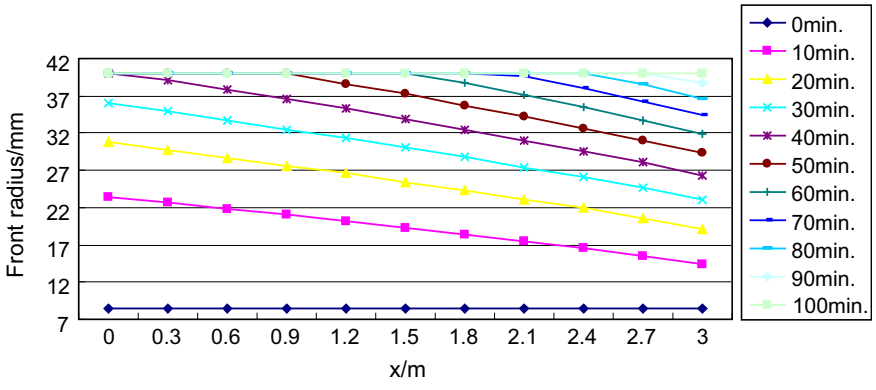

Fig. 7. Solidification front.

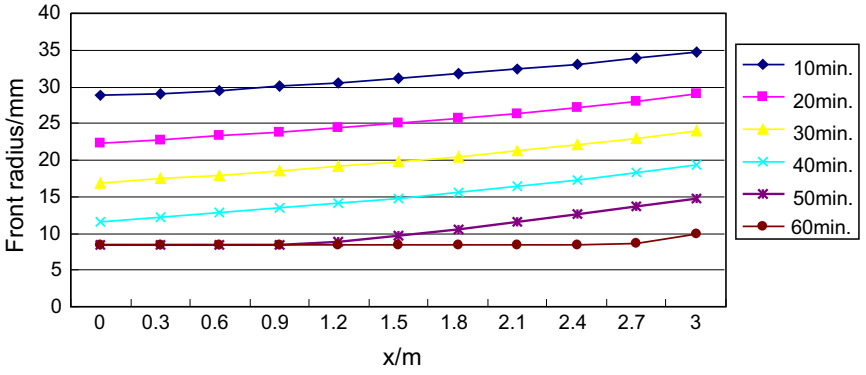

Fig. 8. Melting front.

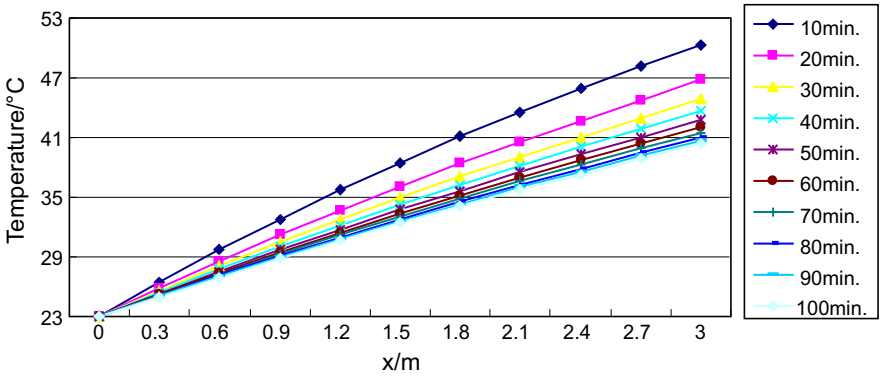

Fig. 9. CHTF temperature distribution.

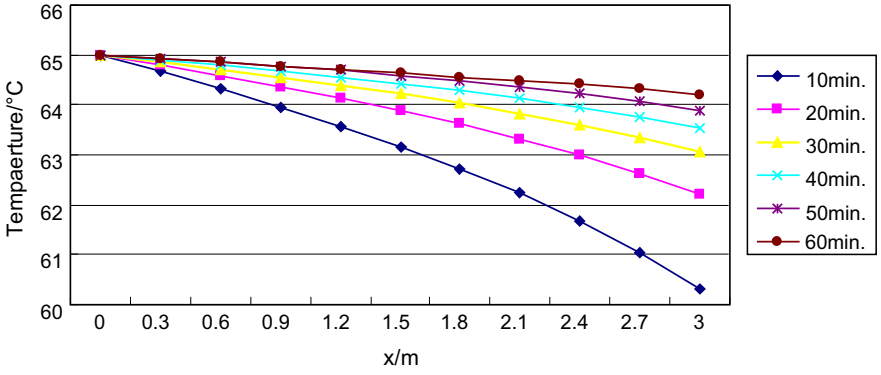

Fig. 10. HHTF temperature distribution.

enhancement of solidification front radius and conductive thermal resistance of PCM, as shown in Fig. 9.

With the inlet fluid temperature at 65 °C, the temperature of HHTF at different axial position increases with time, on the contrary to that of CHTF, as shown in Fig. 10.

3.3.3. Heat transfer rate (Q)

The heat transfer rate (Q) is calculated by the following equation:

$$Q = m_f C_{P,f} |T_{f,out} - T_{in}| \quad (11)$$

where m_f, $C_{P,f}$, $T_{f,out}$ and $T_{f,in}$ denote mass flow rate, average heat capacity, inlet and outlet temperature of CHTF or HHTF, respectively.

As shown in Fig. 11, heat transfer rate during solidification decreases firstly rapidly, then slowly with increasing time. And every 2 °C enhancement of inlet temperature of CHTF results in an average heat recovery rate increase of 0.042 kW.

As shown in Fig. 12, heat transfer rate during melting decreases with increasing time like that of solidification process. The difference is that the inlet temperature of HTF affect heat transfer rate during melting process more

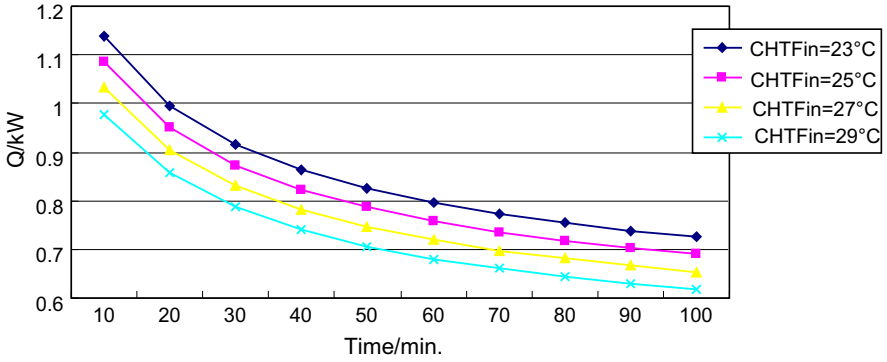

Fig. 11. Heat transfer rate during solidification.

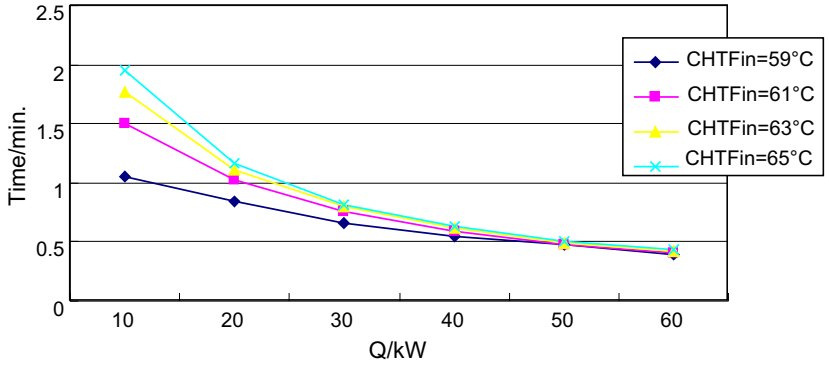

Fig. 12. Heat transfer rate during melting.

and more slightly with increasing time, comparing to the process of solidification.

3.3.4. Time for complete solidification and melting

The effects of the inlet temperature and mass flow rate of HTF on the time for complete solidification and melting are shown in Figs. 13–16, respectively.

As shown in Figs. 13 and 14, inlet temperature of HTF evidently affects the time for complete both solidification and melting. Lower inlet temperature for solidification and higher inlet temperature for melting result in shorter time for complete solidification and melting.

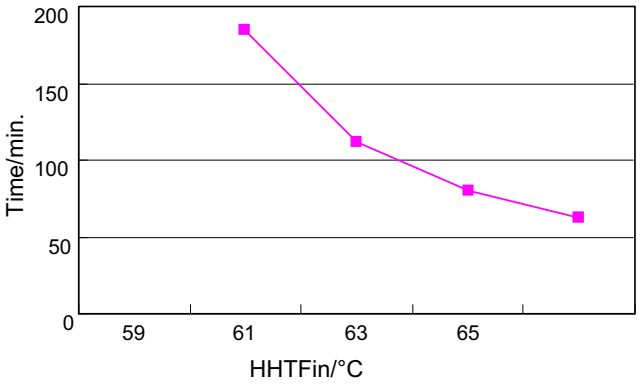

Fig. 14. Time for complete melting.

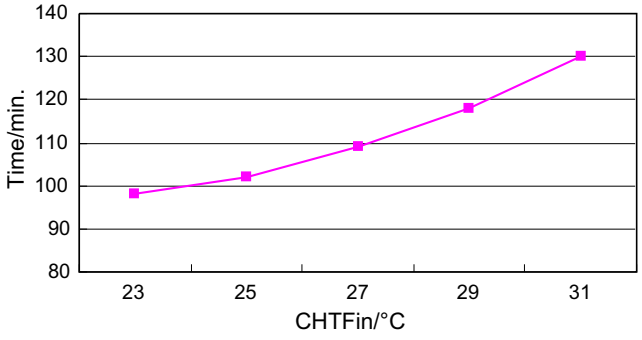

Fig. 13. Time for complete solidification.

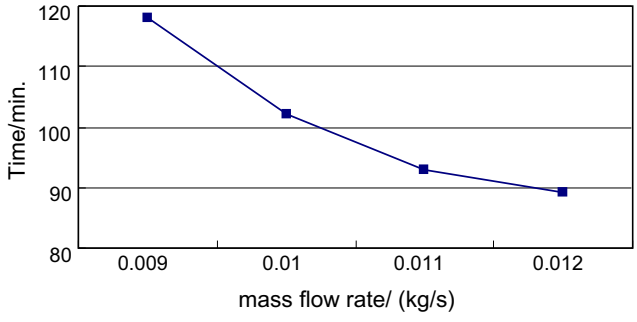

Fig. 15. Time for complete solidification.

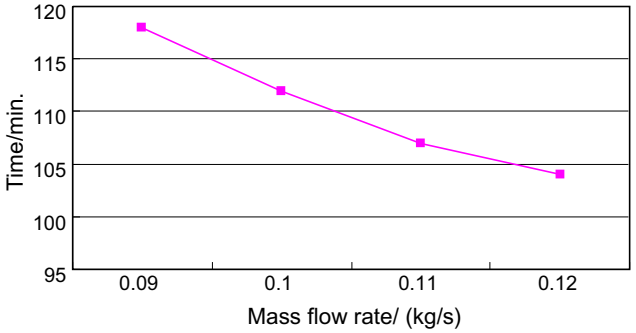

Fig. 16. Time for complete melting.

As can be expected, time for complete solidification and melting strongly depends on mass flow rate of HTF. Larger mass flow rate results in shorter time for complete solidification and melting, as shown in Figs. 15 and 16.

4. Conclusion

A simple numerical method, called temperature & thermal resistance iteration method, has been developed for the analysis of PCM solidification and melting in the triplex concentric tube with PCM filling in the middle channel, with hot heat transfer fluid HHTF flowing outer channel during charging process and cold heat transfer fluid CHTF flowing inner channel during discharging process. This method could be efficiently used for simulation of transient thermal behavior of a latent thermal energy storage unit during charging and discharging.

To test the physical validity of the numerical results, an experimental apparatus has been designed and built by which the effect of the inlet temperature and the flow rate of HHTF/CHTF on the thermal energy storage has been studied. Numerical predictions for both melting and solidification agree quite well with experimental data.

Graphical results including HTF temperature and interface of solid and liquid phase of PCM versus time and axis position, time-wise variation of energy stored/released by the system were presented and discussed. It can be concluded that present work could provide guidelines for thermal performance and design optimization of the latent energy storage unit.

Acknowledgement

The authors would like to acknowledge the financial assistance provided by the Scholar Fund of the Key Laboratory of Enhanced Heat Transfer and Energy Conservation, Ministry of Education, China.

References

Hamada, Y., 2003. Thermal response in thermal energy storage material around heat transfer tubes: effect of additives on heat transfer rates. Solar Energy 75, 317–328.

Banaszek, J., Domanski, R., Rebow, M., et al., 2000. Numerical analysis of the *n*-hexacosane wax–air spiral thermal energy storage unit. Applied Thermal Engineering 20, 323–354.

Al Hallaj, S., Selman, J.R., 2000. A novel thermal management system for electric vehicle batteries using phase change material. Journal of the Electrochemical Society 147 (9), 3231–3236.

Neeper, D.A., 2000. Thermal dynamics of wallboard with latent heat storage. Solar Energy 68 (5), 393–403.

Py, X., Olives, R., Mauran, S., 2001. *N*-Hexacosane/porous-graphite-matrix composite as a high and constant power thermal storage material. International Journal of Heat and Mass Transfer 44, 2727–2737.

Liu, Z., Chung, D.D.L., 2001. Calorimetric evaluation of phase change materials for use as thermal interface materials. Thermochimica Acta 366, 135–147.

Zhang, Y., Faghri, A., 1996. Semi-analytical solution of thermal energy storage system with conjugate laminar forced convection. International Journal of Heat Mass Transfer 39, 717–724.

Ismail, K.A.R., Abugderah, M.M., 2000. Performance of a thermal storage system of the vertical tube type. Energy Conversation & Management 41, 1165–1190.

Zivkovic, B., Fujii, I., 2001. An analysis of isothermal phase change of phase change material within rectangular and cylindrical containers. Solar Energy 70, 51–61.

Sari, A., Kaygusuz, K., 2002. Thermal performance of a eutectic mixture of lauric and stearic acids as pcm encapsulated in the annulus of two concentric pipes. Solar Energy 72, 493–504.

Setterwall, F., 1996. Phase change materials and chemical reaction for thermal energy storage state of the art. Proceedings of the 7th International Conference on Thermal Energy Storage, Sapporo, Japan, pp. 1021–1025.

Kayansayan, N., Ali Acar, M., 2006. Ice formation around a finned-tube heat exchanger for cold thermal energy storage. International Journal of Thermal Sciences 45, 405–418.

Zhang, Y.P., Hu, H.P., Kong, X.D., et al., 1996. Phase Change Energy Storage-Theory and Application. Chinese Science and Technology University Press, Hefei, China, p. 347.

Kang, Y.B., Zhang, Y.P., Zhu, Y.Q., et al., 1999. A simple model for heat transfer analysis of shell-and-tube with phase change material and its performance simulation. International Journal of Heat Mass Transfer 45, 230–236.